Nick Keller* and Aleena Garner*
Optical Capture
13 June 2008
* These authors contributed equally to this work.

**History**

The ability of light to generate a force due to its change in momentum at an interface of media with differing refractive indices has been understood since the time of Kepler and Newton. The idea of radiation pressure was later confirmed by Maxwell, however, outside of astronomical studies where light intensities and distances are very large, no applications for moving matter with radiation pressure existed. Consequently, it was not until the mid-twentieth century, which brought the invention of the laser, that radiation pressure became practically useful in a laboratory setting. The momentum of laser light is capable of generating optical forces that can significantly affect the dynamics of dielectric macro- and micro-particles (Ashkin 1980). The results of such forces allow particles to be trapped and manipulated to measure various parameters. Although, original trapping experiments required two lasers (Ashkin 1980) or one laser and gravity or electrostatic forces to maintain stability (Ashkin & Dziedzic 1971, Ashkin & Dziedzic 1975), by 1986 Ashkin et al. published work on the first single-beam gradient force radiation pressure particle trap. Finally, the popularity of optical trapping in biology to manipulate viruses, bacteria, and other single cells (Ashkin & Dziedzic 1987, Ashkin et al 1987) revealed that the same high numerical aperture (NA) microscope objective could be used for capturing as well as viewing.

Theory

The basic principle behind optical capture is the existence of a scattering force, F_S, a gradient force, F_G, and a restoring force, F_R, and a trapped particle is considered to

experience a net trapping force, $\mathbf{F_T}$. As illustrated in figure 1, the incident laser beam

produces $\mathbf{F_S}$ in the positive z direction, and the Gaussian distribution of the beam creates

$\mathbf{F_G}$ in the positive and negative x directions.
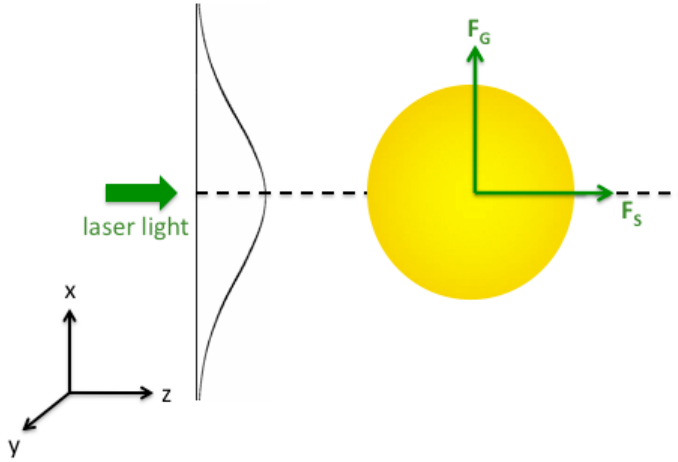
Figure 1. Scattering and Gradient Forces

The incident laser beam is distributed in a Gaussian fashion creating a scattering and gradient force.

$\mathbf{F_R}$ is a result of momentum transfer to the dielectric particle. That is, when a beam of

light, with a certain momentum proportional to its energy and in the direction of its

propagation, is refracted at a dielectric interface, a change in momentum occurs. The

result is a transfer of momentum, of equal magnitude and opposite direction, to the

dielectric particle in order to uphold conservation of momentum. Because

$\mathbf{F} = \partial\mathbf{p}/\partial z$, a force exists, which points in the opposite direction of light. This is

illustrated in figure 2, taken from Smith et al. (1998).
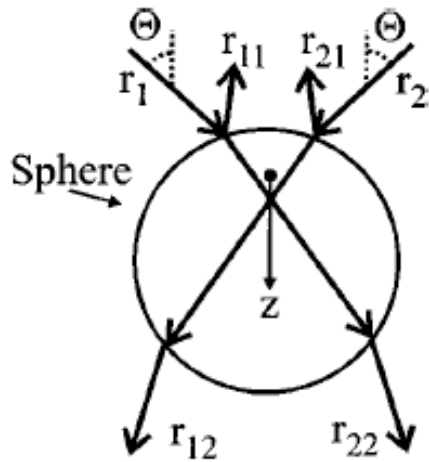
Figure 2. **Restoring Force**

The restoring force results from the change of momentum of light at a dielectric interface.

In this example, r_1 and r_2 are incident rays, r_{11} and r_{21} are reflected rays, and r_{12} and r_{22} are refracted rays. The scattering force generated by the incident light beam is in the positive z direction, while the force due to the refracted rays is in the negative z direction. If the force resulting from the refracted rays is greater than the force resulting from the reflected rays, then a net restoring force will exist and the particle will be stably trapped.

Quantitatively, $\mathbf{F_S}$ and $\mathbf{F_G}$ can be understood by considering a force resulting from an individual incident ray of power P hitting a dielectric particle at an angle θ with momentum per second of n_1P/c. Then the total force on the particle results from the sum of the reflected rays with power PR and the sum of all emergent refracted rays of successively decreasing power PT^2, PT^2R, . . ., PT^2R^n, where R and T are the Fresnel reflection and transmission coefficients of the surface at angle θ (Ashkin 1992).
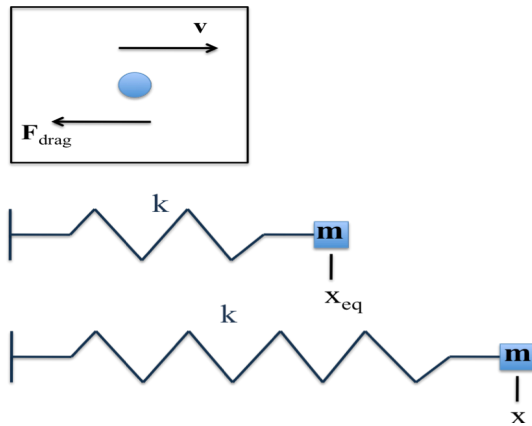
Thus,

$$F_Z = F_S = \frac{n_1 P}{c}$$

$$\left\{ 1 + R \cos 2\theta - \frac{T^2[\cos(2\theta - 2r) + R \cos 2\theta]}{1 + R^2 + 2R \cos 2r} \right\}$$

$$F_Y = F_g = \frac{n_1 P}{c}$$

$$\left\{ R \sin 2\theta - \frac{T^2[\sin(2\theta - 2r) + R \sin 2\theta]}{1 + R^2 + 2R \cos 2r} \right\} \quad \text{(E1, E2)}$$

which is derived in Ashkin 1992 Appendix I.

In this experiment, the trapping force was assumed to be a simple spring with associated force constant k and radial vector, $\bar{x}$. It was also assumed that the trapping force was linear and isotropic, $\vec{F}(x) = -k(\bar{x} - \bar{x}_o)$ (E-3), as shown in figure 3.

Figure 3. Linear model of the trapping force.

X_{eq} is the position of the dielectric microsphere at the focus of the laser trap, and X is the displacement from equilibrium.

The Goal of the Experiment

The goal of the experiment was to first create an optical trap capable of trapping beads in the Mie Regime ($d \approx \lambda$), and second, to use a pair of scanning mirrors to estimate the trapping force constant. As already explained, the trapping or gradient force is conservative and thus a function of the bead's displacement from the bead's equilibrium position. The Stoke's drag force, or frictional force acting on a bead that is moving with velocity, v, with radius, R, in a medium with viscosity, η, is,

$$\vec{F} = -6\pi R\eta\vec{v} \text{ (E-4)}.$$

The conventional experiment that would estimate this force constant would have the particle in some equilibrium position by being trapped in the beam focus. In order to generate a frictional force that would oppose the gradient force, one would use a piezoelectric stage, capable of micrometer displacement. The stage would oscillate at some frequency, giving the particle a velocity in the solution. At threshold, the two forces equal each other and thus Brownian motion takes over, causing the particle to fall out of the trap.

An equivalent scheme has the medium at rest, but the beam focus now oscillating, where the frequency still gives the particle a velocity. Figure 4a attempts to show that both schemes are equivalent. Thus at threshold, $k(x - x_o) = -6\pi R\eta v$ (E-5), where k is the associated force constant of the trapping force.
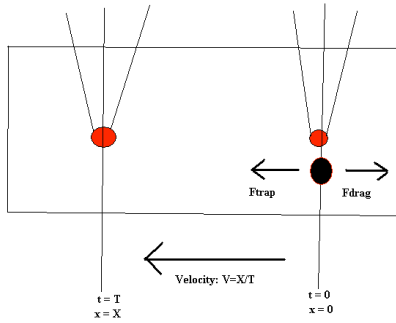
Figure 4a. Our scheme for estimating the trapping force.

The trap has moved in time, T, a distance, X, giving a velocity V, proportional to the drag force, and acting in the opposing direction of the frictional force. Red indicates the trap, black indicates the bead, and arrows indicate vectors.
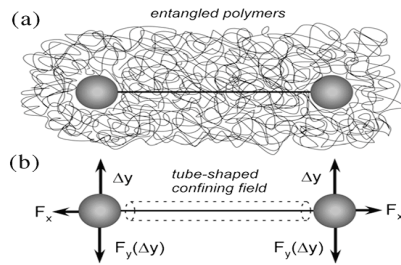

Figure 4b. Conventional scheme for trapping.

Douglas Smith and Rae Robertson held two optically trapped spheres in place. Micrometer displacement, caused by a piezoelectric stage, generated and allowed response forces, acting on the two beads shown, to be measured. (Image taken from Robertson and Smith, 2007)

Experimental Setup

Figure 5 shows the infrared light path of the experiment. The initial light path is as follows: the light beam exiting the laser (IR) reflects off mirror #1 (M1), then off mirror #2 (M2); then enters a pair of scanning mirrors (SM). A single scanning mirror's angle is voltage controlled, allowing alignment via direct current and oscillation via

alternating current, which allows one to vary the drag force acting on the micro sphere. Hence, alignment with the scanning mirrors required two function generates. The beam, after exiting the laser, diverged at an angle of, 0.003 mRad. The beam's diameter was allowed to diverge slightly larger than the back aperture of the objective as required for optimal trapping. Once this diameter was reached, a standard telescope was used, (CV1 and CV2), in order to collimate the laser, which consisted of two converging lenses of focal length, 200 mm. The resulting collimated light completely filled the back aperture of the objective, which subsequently focused the IR beam into a single point onto the plane of micro spheres.   In order to accurately focus the beam into the plane of spheres, an adjustable slide was used for one of the converging lenses. A di-chroic mirror, which transmits IR, and reflects UV, was used in order to image the micro spheres onto a CCD camera. Table 1 includes all the specifications of all the instruments used.
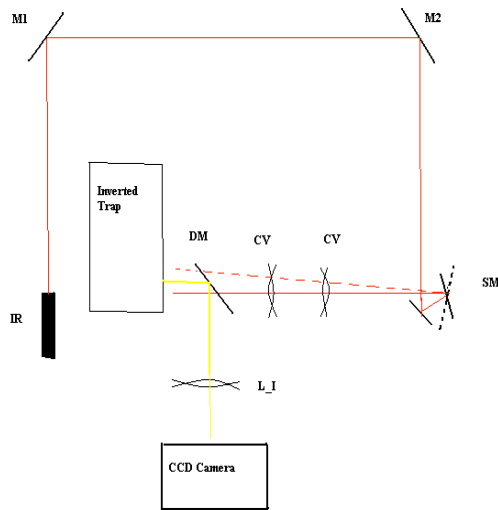
Figure 5. Infrared light path.

 The red line indicates infrared, while the yellow line indicates visible light. The dotted line attempts to show how an oscillation of one of the scanning mirrors alters the IR light path.

The actual optical trap was inverted, as shown in Figure 6, since this was the most efficient way of trapping micro spheres. The actual micro spheres were in dilute solution of de-ionized water of various ratios. For example, the most efficient sample, in terms of being able to center a sphere via an XY stage and trap it, had a water volume of 9 microliters verse a sphere volume of 1 microliter. Referring to Figure 6, the visible light source was a simple bulb driven at 5.V DC via a power source. The two lenses were required to first collimate this light, and then focus it onto the glass sample of micro spheres shown as L1 and L2 with focal lengths of 75.6 mm and 160 mm, respectively. The microscope objective had a working distance of about 0.2 mm and required its tip to be oil immersed in order to focus properly. It also was used as a lens to image the beads onto the CCD camera. The dichroic mirror passed IR light, but reflected visible light, as stated in Table 1.
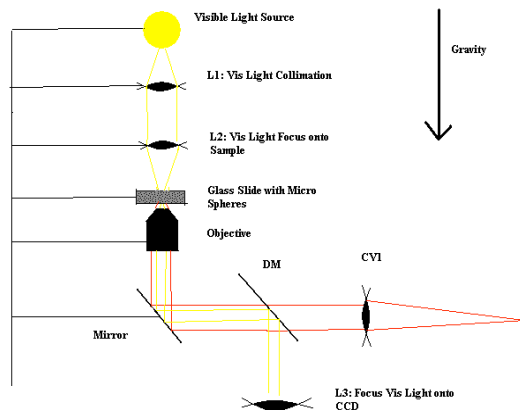
Figure 6. Inverted Optical Trap

M1, M2: Basic mirrors	Reflects %90 in the IR
SM: Scanning mirrors	Angle is DC voltage controlled, working range

|	
	is 2.V; %65 transmission for IR
CV: Converging lens	Converging lens with focal length of 200 mm
DM: Dichroic mirror	90% transmission to IR, while %90 reflection to visible light
L1: Converging lens	Converging lens with focal length of 75.6 mm
Visible light source	Standard 5.V bulb
L2 : Converging lens	Converging lens with focal length of 160 mm
XYZ stage with glass slide containing micro spheres	Cover slip thickness was 0.75 mm
Objective	Wd = 0.2mm; Oil Immersion; NA = 1.26; Back aperture diameter = 5.7 mm

Table 1

Specifications of all instruments used (refer to Figure 5 and 6). IR is infrared light in the range of approximately 700-1000 nm, while visible light has a range of 400-700nm.

Experimental Method

The beam focus had to be focused on the small plate of microspheres. In order to strongly image the beam focus, we used a highly concentrated solution of microspheres

as to reflect the IR radiation efficiently. Since the dichroic had a %10 reflection coefficient in the IR, we could see the scattered light. With the objective in place just above sample, we varied the Z-stage such that a bright image showed up on the TV as shown in Figure 7. The reflections to the left of the bright focus caused a problem in trapping since this causes the actual trap to lose intensity. This problem could not be avoided.
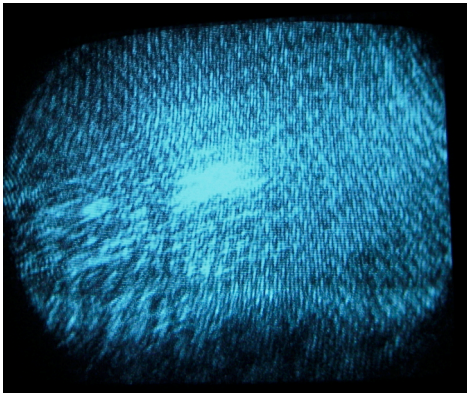
Figure 7

 TV image of the focus of the beam on a highly concentrated sample of microspheres, d = 2.5 micrometers.

Next, we tried to image both the micro spheres and beam focus, which was done varying L_I, the lens in front of the CCD in Figure 5. Note that if the Z-stage was varied at all in order to better focus the sphere on the TV, the focal plane of the beam no longer coincided with focal plane of the beads, as shown in Figure 8.


Sample with
Micro Beads

Objective
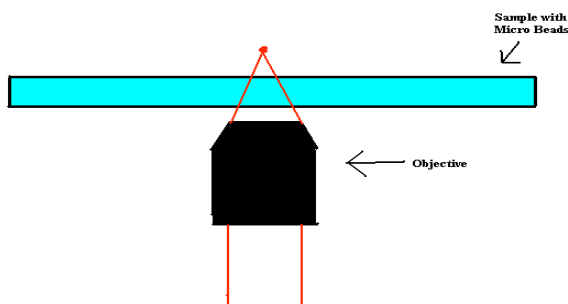
Figure 8.

Complication arising if Z-stage is moved to better resolve the microspheres.

Experimental Results

As already stated, we wanted to trap a sphere with both a stationary mirror and a pair of scanning mirrors. Stable trapping with a stationary mirror was observed, however trapping with the scanning mirrors was not observed. Although we were able to image both the beam focus and the spheres with assurance that both spheres and beam focus were in the same plane, a stable trap could not be established. We speculate that the beam focus was not intense enough, implying the gradient force not strong enough. Power loss was observed along the optical path consisting of the beam collimator (CV in Figure 5) since small reflections were observed as the beam passed both lenses.

Figure 9 shows a sphere with no IR radiation, while Figure 10 shows an optically trapped sphere with a stationary mirror. Since, the Z-stage could not be moved, 2D trapping was only possible. Trapping was done with sphere diameters of 1 and 2 micrometers.
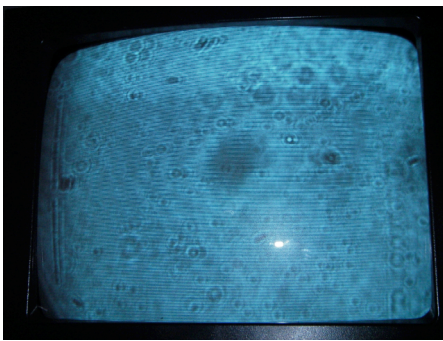
Figure 9.

Imaged sphere with no IR radiation.
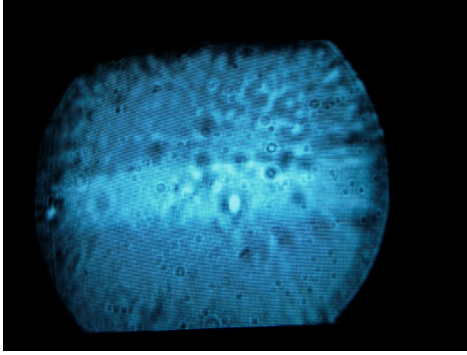
Figure 10.

 Imaged optically trapped sphere with a stationary mirror.

Conclusion

By being able to build the experiment from scratch, and having no experimental optical experience, we believe the experiment was a success. Given more time, we most likely could have been able to trap with the pair of scanning mirrors. Optimal trapping occurs when alignment is exact, thereby guaranteeing the maximum possible gradient force. One should always check the transmission coefficient for each lens and mirror used as to insure enough intensity is being transmitted. The method proposed in trapping the spheres was efficient.

References

1. Ashkin, A., and J. M. Dziedzic. 1971. Optical levitation by radiation pressure. Appl. Phys. Lett. 19:283-285.

2. Ashkin, A., and J. M. Dziedzic. 1975. Optical levitation of liquid drops by radiation pressure. Science (Wash. DC). 187:1073-1075.

3. Ashkin, A. 1980. Applications of Laser Radiation Pressure. Science, New Series. 210: 1081-1088.

4. Ashkin, A., Dziedzic, J.M., Bjorkholm, J.E., and Chu, S. Observation of a single-beam gradient force optical trap for dielectric particles. Optics Letters. 11: 288-290

5. Ashkin, A., Dziedzic, J.M. 1987. Optical trapping and manipulations of viruses and bacteria. Science. 20;235(4795):1517-1520.

6. Ashkin, A. Dziedzic, J.M., Yamane, T. 1987. Optical trapping and manipulation of single cells using infrared laser beams. Nature. 24-31;330(6150):769-771.

7. Ashkin, A. 1992. Forces of a single-beam gradient laser trap on a dielectric sphere in the ray optics regime. Biophys. J. 61:569-582.

9. Robertson, R.M. and Smith, D.E. 2007. Direct measurement of the intermolecular forces confining a single molecule in an entangled polymer solution. Physical Review Letters. 99(12):1-4

8. Smith, S.P., Bhalotra, S.R., Brody, A.L., Brown, B.L., Boyda, E.K., Prentiss, M. 1998. Inexpensive optical tweezers for undergraduate laboratories. American Maerican Journal of Physics. 67(1): 26-35.